3. R. J. Brodd *et al.*, *J. Electrochem. Soc.* **151**, K1 (2004).
4. G. Woolfe, *Batteries Energy Storage Technol.* **3**, 107 (2005).
5. J. N. Barisci, G. G. Wallace, D. R. MacFarlane, R. H. Baughman, *Electrochem. Commun.* **6**, 22 (2004).
6. A. Rudge, J. Davey, I. Raistrick, S. Gottesfeld, J. P. Ferraris, *J. Power Sources* **47**, 89 (1994).
7. E. Frackowiak, F. Beguin, *Carbon* **39**, 937 (2001).
8. J. Gamby, P. L. Taberna, P. Simon, J. F. Fauvarque, M. Chesneau, *J. Power Sources* **101**, 109 (2001).
9. G. Salitra, A. Soffer, L. Eliad, Y. Cohen, D. Aurback, *J. Electrochem. Soc.* **147**, 2486 (2000).
10. F. Beguin, E. Frackowiak, in *Nanomaterials Handbook*, Y. Gogotsi, Ed. (CRC Press, Boca Raton, FL, 2006), pp. 713–737.
11. H. Zhou, S. Zhu, M. Hibino, I. Honma, *J. Power Sources* **122**, 219 (2003).
12. R. H. Baughman, A. A. Zakhidov, W. A. de Heer, *Science* **297**, 787 (2002).
13. G. Yushin, A. Nikitin, Y. Gogotsi, in *Nanomaterials Handbook*, Y. Gogotsi, Ed. (CRC Press, Boca Raton, FL, 2006), pp. 237–280.
14. Y. Gogotsi *et al.*, *Nat. Mater.* **2**, 591 (2003).
15. R. K. Dash, G. Yushin, Y. Gogotsi, *Micropor. Mesopor. Mat.* **86**, 50 (2005).
16. Y. Gogotsi *et al.*, *J. Am. Chem. Soc.* **127**, 16006 (2005).
17. J. Chmiola *et al.*, *Electrochem. Solid-State Lett.* **8**, A357 (2005).
18. J. Chmiola, G. Yushin, R. Dash, Y. Gogotsi, *J. Power Sources* **158**, 765 (2006).
19. A. Janes, L. Permann, M. Arulepp, E. Lust, *Electrochem. Commun.* **6**, 313 (2004).
20. P. Zetterstrom *et al.*, *J. Phys. Condens. Matter* **17**, 3509 (2005).
21. Materials and methods are available as supporting material on *Science* Online.
22. G. Laudisio *et al.*, *Langmuir*, in press.
23. P. L. Taberna, P. Simon, J. F. Fauvarque, *J. Electrochem. Soc.* **150**, A292 (2003).
24. M. Endo *et al.*, *J. Electrochem. Soc.* **148**, A910 (2001).
25. H. Shi, *Electrochim. Acta* **41**, 1633 (1996).
26. C. Vix-Guterl *et al.*, *Carbon* **43**, 1293 (2005).
27. R. de Levie, A. Vogt, *J. Electroanal. Chem.* **341**, 353 (1992).
28. J. Dzubiella, J. P. Hansen, *J. Chem. Phys.* **122**, 234706 (2005).
29. J. M. Di Leo, J. Maranon, *J. Mol. Struct.* **729**, 53 (2004).
30. M. Carrillo-Tripp, H. Saint-Martin, I. Ortega-Blake, *Phys. Rev. Lett.* **93**, 168104 (2004).
31. T. Ohkubo *et al.*, *J. Am. Chem. Soc.* **124**, 11860 (2002).
32. We thank R. K. Dash and D. Berrigan (Drexel University) for experimental help and J. E. Fischer (University of Pennsylvania) for numerous helpful discussions. J.C. was supported by an NSF IGERT Fellowship. C.P. was supported by Delegation Generale pour l'Armement (DGA) in France. This work was partially supported by Arkema, France. TEM was performed at the Regional Nanotechnology Facility at the University of Pennsylvania. Raman microspectroscopy was performed at the Materials Characterization Facility at Drexel University with the help of Z. Nikolov.

Supporting Online Material

www.sciencemag.org/cgi/content/full//1132195/DC1
Materials and Methods
Figs. S1 to S6
References

7 July 2006; accepted 10 August 2006
Published online 17 August 2006;
10.1126/science/1132195
Include this information when citing this paper.

Oxygen Isotope Variation in Stony-Iron Meteorites

R. C. Greenwood,[1]* I. A. Franchi,[1] A. Jambon,[2] J. A. Barrat,[3] T. H. Burbine[4]

Asteroidal material, delivered to Earth as meteorites, preserves a record of the earliest stages of planetary formation. High-precision oxygen isotope analyses for the two major groups of stony-iron meteorites (main-group pallasites and mesosiderites) demonstrate that each group is from a distinct asteroidal source. Mesosiderites are isotopically identical to the howardite-eucrite-diogenite clan and, like them, are probably derived from the asteroid 4 Vesta. Main-group pallasites represent intermixed core-mantle material from a single disrupted asteroid and have no known equivalents among the basaltic meteorites. The stony-iron meteorites demonstrate that intense asteroidal deformation accompanied planetary accretion in the early Solar System.

The terrestrial planets formed by the collision and merger of smaller bodies, over a period lasting up to 100 million years (My) after Solar System formation (*1*). The final stage of this process was marked by giant impacts that resulted in large-scale planetary melting (*2*). As a consequence of their protracted formation histories, and subsequent geological reprocessing, the initial stages of planetary accretion are not recorded by these larger bodies. In contrast, asteroids preserve a record of the earliest stages of planetary growth. Thus, W isotopic analysis of iron meteorites (*3*) and Mg isotope studies of basaltic meteorites (*4*) indicate that the earliest asteroids accreted within 1 My of Solar System formation and, due to the presence of live ^{26}Al, rapidly underwent near-total melting.

However, the usefulness of asteroidal material in understanding the earliest stages of planetary formation is hindered by the fragmentary nature of the meteorite record. As a result, we are unable to say how many asteroids are represented in our meteorite collections (*5*). Oxygen isotope analysis is one method that has proven useful in understanding the relationships between the various meteorite sample suites (*6*). The melting event that caused the early-formed asteroids to segregate into a metal-rich core and silicate-rich mantle and crust also homogenized their oxygen isotopes (*7*). The later evolution of these bodies would be by mass-dependent fractionation processes, so that samples derived from the same source asteroid define a single mass fractionation line (slope ≈ 0.52) on a three-isotope diagram (*6*, *8*). Meteorite samples from melted asteroids are collectively referred to as differentiated achondrites.

One limitation with this technique results from the small-scale oxygen isotope variation displayed by many groups of differentiated achondrites (*6*). Thus, main-group pallasites, mesosiderites, and the howardite-eucrite-diogenite suite (HEDs) (*9*) all plot within the same area on an oxygen three-isotope diagram (*6*) and could, in theory, have come from a single asteroid. However, mineralogical and textural evidence indicates that these groups formed in distinct settings, with the HEDs and mesosiderites coming from the outer crust of an asteroid, whereas the main-group pallasites formed deep within their parent body (*10*). Because reflectance spectra indicate that HEDs are from the relatively intact asteroid 4 Vesta (*11*), the main-group pallasites must come from a separate source (*10*). To address the problem of such overlapping oxygen isotope variation, we have undertaken a detailed study of the main-group pallasites and mesosiderites by laser-assisted fluorination (*12*). The high analytical precision of this technique enables the offset between parallel mass fractionation lines to be measured to within ±0.02‰ (*12*) and therefore has the potential to resolve the overlaps seen in the differentiated achondrites.

The results of oxygen isotope analyses (*13*) unambiguously resolve the mesosiderites from the main-group pallasites; thus, each group defines a distinct linear array on an oxygen isotope variation diagram (Fig. 1). The mean Δ^{17}O (*8*) value is –0.183 ± 0.018 (2σ) for the main-group pallasites and –0.245 ± 0.020 (2σ) for the mesosiderites (*13*).

The mean Δ^{17}O value for the mesosiderites is indistinguishable from the previously determined HED value of –0.238 ± 0.014 (*7*). Furthermore, if data from laser-assisted fluorination studies of the HEDs are combined (*7*, *14*), the range in δ^{18}O values for the mesosiderites and HEDs are virtually identical (Fig. 1). It has long been known that the silicate portion of the mesosiderites and the various lithologies of the HED suite show strong mineralogical and geochemical similarities (*10*).

[1]Planetary and Space Sciences Research Institute, Open University, Walton Hall, Milton Keynes, MK7 6AA UK. [2]Laboratoire Magmatologie et Géochimie Inorganique et Expérimentale, Université Pierre et Marie Curie, CNRS UMR 7047 case 110, 4 place Jussieu, 75252 Paris Cedex 05, France. [3]Université de Bretagne Occidentale–Universitaire Européen de la Mer, CNRS UMR 6538 (Domaines Océaniques), place Nicolas Copernic, F-29280 Plouzané Cedex, France. [4]Department of Astronomy, Mount Holyoke College, South Hadley, MA 01075, USA.

*To whom correspondence should be addressed. E-mail: r.c.greenwood@open.ac.uk

This evidence, combined with their similar oxygen isotope variation, suggests that both groups may have a common origin. However, a single source for these groups is not widely accepted, objections cited being (i) lack of remote sensing evidence that mesosiderites are present on Vesta (*15*), (ii) lack of metal-rich clasts in howardites (*10*, *16*), (iii) paucity of olivine in the HEDs (*10*), and (iv) silicate clast populations in the two groups that are not identical, although geochemically similar (*10*, *16*).

On closer scrutiny, these arguments are less persuasive. Remote sensing does not indicate the presence of mesosiderites on Vesta, simply because metallic iron does not have any spectral features in the visible and near-infrared. Howardites containing mesosiderite-like clasts have now been identified (*17*) and, in addition, platinum-group element signatures in both brecciated eucrites and mesosiderites show strong similarities (*18*). Paucity of olivine in HEDs is not a strong argument in favor of separate parent bodies. Olivine is an accessory phase in HEDs (*10*), and olivine-rich diogenites, with up to 45% modal olivine, have now been identified (*19*). It is well understood that the metal-silicate mixing event that formed the mesosiderites took place at high temperatures, with the metal fraction being essentially molten (*20*). Comparing these altered mesosiderite clasts with unaltered HED material is not in itself a compelling argument for separate source asteroids (*10*, *16*), because local-scale metal-silicate mixing processes on a single parent body could equally explain these differences.

Vesta has been proposed as the parent body of the HEDs, mainly due to its distinctive reflectance spectrum, which is close in structure to the laboratory-measured HED spectra (*10*, *11*). The link between Vesta and the HEDs has been strengthened by the discovery of smaller asteroids known as Vestoids, with Vesta-like spectra and apparently derived from it by impact processes (*11*). A number of Vestoids occupy positions in the asteroid belt between Vesta and the 3:1 meteorite-supplying resonance (~2.5 astronomical units) and hence solve the problem of how fragments of Vesta can be placed into Earth-crossing orbit (*11*). If mesosiderites are also derived from Vesta, they are likely to be exposed at the asteroid's surface and should be detectable using the instrument package on the NASA Dawn discovery mission (*21*).

Recent isotopic dating is broadly consistent with a single source for the HEDs and mesosiderites. Mg isotopes indicate that initial formation of the HEDs and mesosiderites was contemporaneous, occurring <1 My after Solar System formation (*4*). Evidence that Mn/Cr fractionation in the Vaca Muerta mesosiderite took place ~2 Myr later than in the HEDs (*20*) appears to be at odds with evidence that Al/Mg fractionation occurred slightly later in the HEDs than in Vaca Muerta (*4*). These differences may reflect isotopic disturbance during metal-silicate mixing (*4*, *20*). There is also uncertainty concerning the timing of the metal-silicate mixing event, with Cr isotopes indicating a younger age (>20 My after Solar System formation) than W isotopes (~5 My after Solar System formation) (*20*). This again may result from isotopic disturbance during metal-silicate mixing (*20*).

The origin of mesosiderites remains controversial, with a diverse range of models put forward to explain their genesis (*15*, *16*, *20*, *22*, *23*). They may have formed when the molten metal core of a denuded asteroid impact-mixed with the outer layers of a second differentiated body (*16*, *20*, *22*). Alternatively, the mesosiderites are viewed as the products formed when an asteroid with a molten core was disrupted and subsequently reaccreted (*23*). If mesosiderites and HEDs are both derived from the relatively intact asteroid Vesta, total parent-body disruption and subsequent reaccretion appears unlikely (*23*). Thus, impact of a molten asteroid core into the surface layers of a second differentiated asteroid is the more plausible model to explain mesosiderite formation (*16*, *20*, *22*). Evidence indicating that mesosiderites cooled rapidly at high temperatures (~10^5°C/My in the range 850° to 1150°C) (*23*), but slowly at lower temperatures (~0.03° to 1°C/My in the range 400° to 250°C) (*23*), possibly due to the formation of an ejecta blanket, appears compatible with this model.

Close encounters between asteroids would have been common events in the early Solar System and could result in the smaller of the bodies being left in a deformed state, having lost much of its crust and mantle (*24*). Pressure release associated with such gravitational unloading may have caused remelting of the remaining core (*24*). Given the extent of collisional encounters in the early Solar System (*1*, *24*), processes similar to those that formed the mesosiderites must have been relatively commonplace events. The unique aspect of the mesosiderites is that the evidence for these processes has been preserved and not obliterated by later collisions and mergers; this is possibly because their formation was a relatively late-stage event (*20*).

It is clear from the results of this study that the main-group pallasites are derived from an asteroidal source distinct from that of either the mesosiderites or the HEDs (Fig. 1). The main-group pallasite mean $\Delta^{17}O$ value of –0.183 ± 0.018 (2σ) is unique and does not correspond to any known group of basaltic meteorites. Main-group pallasites must therefore sample a disrupted differentiated asteroid, in which much of the outer crustal material was removed.

There is general agreement that main-group pallasites are samples from the core-mantle boundary of a differentiated asteroid (*25*, *26*). Because metal sinks to form the core of a molten asteroid and olivine would be the major constituent of the lower mantle, this model appears reasonable (*10*). However, two outstanding problems remain: (i) main-group pallasites seem overabundant relative to the small volume of the core-mantle interface and (ii) because of their large difference in density, olivine and liquid metal should unmix rapidly (*10*).

The primary angular olivine texture of main-group pallasites (*25*, *26*) is generally regarded as the product of a major impact event, in which olivine-rich lower mantle material was catastrophically driven into the underlying partially molten core (*10*, *25*, *26*). This was followed by rapid solidification of the metal melt, thus preventing any subsequent unmixing (*25*, *26*). In consequence, pallasites should no longer be regarded as mere samples of an asteroid's core-mantle boundary but rather as an impact-generated lithology composed of intermixed core and mantle material. This explains the apparent overabundance of main-group pallasites (*10*), because an impact-generated mixing zone would have a much greater volume than a gravity-produced core-mantle boundary layer,

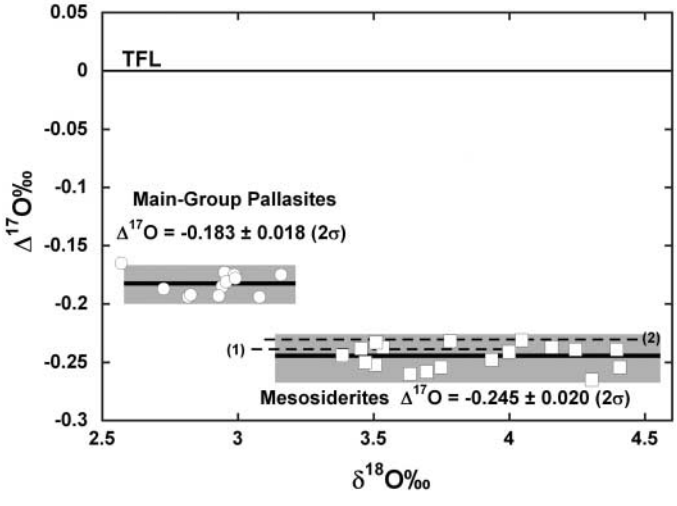

Fig. 1. Oxygen isotope variation in mesosiderites and main-group pallasites. Analytical data for individual samples is given in table S1. Solid lines show the mean $\Delta^{17}O$ value for both the mesosiderites and main-group pallasites. For clarity, error bars for individual analysis have been omitted. However, the gray-shaded boxes depict the 2σ error on the mesosiderite and main-group pallasite population $\Delta^{17}O$ and $\delta^{18}O$ mean values. Open squares, mesosiderite analyses; open circles, pallasite analyses; TFL, terrestrial fractionation line. Line 1 is the eucrite fractionation line of (*7*); line 2 shows the range of HED values obtained by (*14*).

which is essentially just a two-dimensional interface. The lack of basaltic meteorites with a $\Delta^{17}O$ value equivalent to the main-group pallasites suggests that the outer crustal layers were removed from the parent asteroid. This may have taken place during the pallasite-forming impact event itself. If loss of surface material took place as the result of a collisional encounter (*24*), the extent of silicate loss appears to have been much less in the pallasites than mesosiderites, because the former show no evidence for remelting of the metal core.

Metal in main-group pallasites is compositionally similar to that in the IIIAB irons, such that both groups are probably derived from the same asteroid (*26*). W isotope dating of IIIAB irons indicates that the metal-silicate segregation event that formed them occurred extremely early (<1 My after Solar System formation) (*3*). Mn-Cr dating is consistent with an early formation age for main-group pallasites (*10*), although the isotope systematics show evidence of disturbance, probably in part as a consequence of impact-related processes (*27*). The cooling rates recorded by main-group pallasites also reflect impact-related processes. Thus, cooling at high temperatures (~1100°C) took place 10^6 times faster than at lower temperatures (~1°C/My at 800° to 400°C) (*27*). The higher rates may have resulted from impact-driven mixing of partially molten metal and solid silicate mantle material, whereas slower cooling may reflect postimpact burial (*25*).

The results presented here demonstrate that pallasites and mesosiderites are derived from distinct asteroidal sources. Like the HEDs, mesosiderites are probably samples from the asteroid 4 Vesta, a conclusion that can be tested by the NASA Dawn Mission (*21*). It is also clear from these results that extensive asteroidal deformation was an important process during the early stages of planetary formation. Recent observations suggest that such collisional reprocessing of planetesimals may also be a significant feature of extrasolar planetary systems, such as the solar-type star BD+20 307 (*28*).

References and Notes

1. S. J. Weidenschilling, *Space Sci. Rev.* **92**, 295 (2000).
2. D. C. Rubie, C. K. Gessmann, D. J. Frost, *Nature* **429**, 58 (2004).
3. A. Markowski, G. Quitté, A. N. Halliday, T. Kleine, *Earth Planet. Sci. Lett.* **242**, 1 (2006).
4. M. Bizzarro, J. A. Baker, H. Haack, K. L. Lundgaard, *Astrophys. J.* **632**, L41 (2005).
5. T. H. Burbine, T. J. McCoy, A. Meibom, B. Gladman, K. Keil, in *Asteroids III*, W. F. Bottke Jr., A. Cellino, P. Paolicchi, R. P. Binzel, Eds. (Univ. Arizona Press, Tucson, AZ, 2002), pp. 653–667.
6. R. N. Clayton, T. K. Mayeda, *Geochim. Cosmochim. Acta* **60**, 1999 (1996).
7. R. C. Greenwood, I. A. Franchi, A. Jambon, P. C. Buchanan, *Nature* **435**, 916 (2005).
8. Oxygen has three naturally occurring stable isotopes, ^{16}O, ^{17}O, and ^{18}O, with natural abundances of ~99.762%, 0.038%, and 0.200%, respectively (*29*). Oxygen isotope variation is reported in terms of per mil (‰) differences in the ratios $^{18}O/^{16}O$ and $^{17}O/^{16}O$ relative to the VSMOW (Vienna Standard Mean Ocean Water) standard expressed as $\delta^{18}O = [(^{18}O/^{16}O)_{sample}/(^{18}O/^{16}O)_{VSMOW}) - 1]1000$ and similarly for $\delta^{17}O$ using $^{17}O/^{16}O$ ratio of the sample and VSMOW. Oxygen isotope values are conventionally plotted on a "three-isotope plot" with $\delta^{18}O$ along the *x* axis and $\delta^{17}O$ along the *y* axis. On such a plot, rocks and waters on Earth define a single line with a slope close to 0.52, known as the terrestrial fractionation line. Deviations from this line are conventionally expressed as: $\Delta^{17}O = \delta^{17}O - 0.52\ \delta^{18}O$; however, this is in fact an approximation of a power law function, and hence the more accurate linearized format is used here: $\Delta^{17}O = 1000\ \ln[1+(\delta^{17}O/1000)] - \lambda 1000\ \ln[1 + (\delta^{18}O/1000)]$, where $\lambda = 0.5247$ (*29*).
9. Main-group pallasites and mesosiderites are composed of subequal amounts of Fe-Ni metal and silicate material. The two groups are texturally and compositionally quite distinct. Main-group pallasites consist of large olivine crystals enclosed in Fe-Ni metal, whereas mesosiderites are complex breccias of metal-rich clasts, basaltic, gabbroic, and rarer pyroxenitic fragments enclosed in a fine-grained metal-silicate matrix. HEDs are a suite of basaltic and related coarser-grained igneous meteorites that are believed to be samples of the outer crust of asteroid 4 Vesta (*10*).
10. D. W. Mittlefehldt, T. J. McCoy, C. A. Goodrich, A. Kracher, in *Planetary Materials*, J. J. Papike, Ed. (*Min. Soc. Am. Reviews in Mineralogy* 36), 4-1 (1998).
11. T. H. Burbine *et al.*, *Meteorit. Planet. Sci.* **36**, 761 (2001).
12. M. F. Miller, I. A. Franchi, A. S. Sexton, C. T. Pillinger, *Rapid Commun. Mass Spectrom.* **13**, 1211 (1999).
13. Materials and methods are available as supporting material on *Science* Online.
14. U. Wiechert, A. N. Halliday, H. Palme, D. Rumble, *Earth Planet. Sci. Lett.* **221**, 373 (2004).
15. R. H. Hewins, *J. Geophys. Res.* **88** (Supplement), B257 (1983).
16. A. H. Rubin, D. W. Mittlefehldt, *Icarus* **101**, 201 (1993).
17. M. T. Rosing, H. Haack, *Lunar Planet. Sci. Conf.* **35**, 1487 (2004).
18. A. Yamaguchi, C. Okamoto, M. Ebihara, *Lunar Planet. Sci. Conf.* **37**, 1678 (2006).
19. The following olivine-rich diogenites have been identified in recent years: GRA 98108, NWA 1459, NWA 1877, NWA 2629, and NWA 2286. Details of each of these specimens is available on the Meteoritical Bulletin Database, http://tin.er.usgs.gov/meteor.
20. M. Wadhwa, A. Shukolyukov, A. M. Davis, G. W. Lugmair, D. W. Mittlefehldt, *Geochim. Cosmochim. Acta* **67**, 5047 (2003).
21. C. T. Russell *et al.*, *Planet. Space Sci.* **52**, 465 (2004).
22. J. T. Wasson, A. E. Rubin, *Nature* **318**, 168 (1985).
23. R. D. Scott, H. Haack, S. G. Love, *Meteorit. Planet. Sci.* **36**, 869 (2001).
24. E. Asphaug, C. B. Agnor, Q. Williams, *Nature* **439**, 155 (2006).
25. E. R. D. Scott, G. J. Taylor, *Lunar Planet. Sci. Conf.* **21**, 1119 (1990).
26. J. T. Wasson, B.-G. Choi, *Geochim. Cosmochim. Acta* **67**, 3079 (2003).
27. T. Tomiyama, G. R. Huss, *Lunar Planet. Sci. Conf.* **36**, 2071 (2005).
28. I. Song, B. Zuckerman, A. J. Weinberger, E. E. Becklin, *Nature* **436**, 363 (2005).
29. M. F. Miller, *Geochim. Cosmochim. Acta* **66**, 1881 (2002).

30. We would like to thank M. Farmer, who supplied samples of Dong Ujimqin QI; B. Zanda (Muséum National d'Histoire Naturelle, Paris) and C. Smith (Natural History Museum, London) for providing mesosiderite and pallasite samples; and Jenny Gibson (Open University) for help with various aspects of oxygen isotope analysis. We would like to thank three anonymous reviewers for their comments. This study was supported by a PPARC rolling grant to PSSRI, Open University. T.H.B. acknowledges support from NASA Cosmochemistry grant NAG5-12848.

Supporting Online Material

www.sciencemag.org/cgi/content/full/1128865/DC1
Materials and Methods
Figs. S1 and S2
Table S1

18 April 2006; accepted 27 July 2006
Published online 24 August 2006;
10.1126/science.1128865
Include this information when citing this paper.

Self-Healing Pulse-Like Shear Ruptures in the Laboratory

George Lykotrafitis, Ares J. Rosakis,* Guruswami Ravichandran

Models predict that dynamic shear ruptures during earthquake faulting occur as either sliding cracks, where a large section of the interface slides behind a fast-moving rupture front, or self-healing slip pulses, where the fault relocks shortly behind the rupture front. We report experimental visualizations of crack-like, pulse-like, and mixed rupture modes propagating along frictionally held, "incoherent" interfaces separating identical solids, and we describe the conditions under which those modes develop. A combination of simultaneously performed measurements via dynamic photoelasticity and laser interferometry reveals the rupture mode type, the exact point of rupture initiation, the sliding velocity history, and the rupture propagation speed.

A central issue in the modeling of earthquake rupture is the duration of slip at a point on the fault as compared to the duration of the rupture of the entire fault (*1*). In the classical crack-like mode of shear rupture (*2*), the slip duration at a point (rise time) is a considerable fraction of the overall rupture propagation time. In other words, the duration of the ground shaking, witnessed locally by an observer, is comparable to the overall duration of the earthquake. This mode has been generated in several numerical simulations of spontaneous rupture, when a rate-independent friction law was implemented (*3*–*7*). However, inversions of seismic data for slip histories from well-recorded events indicate that the duration of slip at a point on the fault is often one order of magnitude shorter

Graduate Aeronautical Laboratories, California Institute of Technology, Pasadena, CA 91125, USA.

*To whom correspondence should be addressed. E-mail: Rosakis@aero.caltech.edu